

Fluorogenic Recognition of Zn^{2+} , Al^{3+} and F^{-} Ions by a New Multi-Analyte Chemosensor Based Bisphenol A-Quinoline

Serkan Erdemir¹ · Ozcan Kocycigit¹ · Sait Malkondu¹

Received: 13 February 2015 / Accepted: 5 March 2015 / Published online: 18 March 2015
© Springer Science+Business Media New York 2015

Abstract A new available multi-analyte fluorescent sensor based on a bisphenol A-quinoline conjugate (**BFQ**) was synthesized in two facile steps and was characterized systematically. **BFQ** exhibited an effectively selective and sensitive recognition toward Zn^{2+} and Al^{3+} cations in EtOH- H_2O ($\nu/\nu=9/1$) over other cations and F^{-} anion in CH_3CN over other anions with remarkably enhanced fluorescent intensities. According to the quantum yield (Φ) measurements, **BFQ**- Zn^{2+} , **BFQ**- Al^{3+} and **BFQ**- F^{-} complexes showed 16, 22 and 30 times higher Φ values than **BFQ**, respectively. The complexation properties of **BFQ** with Zn^{2+} , Al^{3+} and F^{-} ions were also examined by 1H NMR titration experiments.

Keywords Bisphenol A · Quinoline · Fluorometric · Turn on · Chemosensor

Introduction

The development of fluorescent chemosensors for anions and cations of biologically important and environmental pollutant is always important and generally involves the design and synthesis of fluorophore containing more than one binding sites and a signaling unit. Sensing multiple analytes with a single chemosensor is a challenging task. It involves eliciting

Electronic supplementary material The online version of this article (doi:10.1007/s10895-015-1557-6) contains supplementary material, which is available to authorized users.

✉ Serkan Erdemir
serdemir82@gmail.com

¹ Science Faculty, Department of Chemistry, Selcuk University, Konya 42031, Turkey

different responses by the molecule in the presence of different analytes [1–4]. An important natural metal element, zinc, is the second most abundant metal ion and is actively involved in diverse biological activities, such as structural and catalytic cofactors, neural signal transmitters or modulators, regulators of gene expression and apoptosis [5, 6]. Minute quantities of zinc are necessary for the living organism, but excessive amounts may damage the organism [7–9]. Also, the design of a highly selective and sensitive fluorescence sensor for Zn^{2+} detection without interference from other metal ions, especially Cd^{2+} , is one of the most important objectives since cadmium is in the same group of the periodic table and has similar properties. Aluminum is the third most prevalent (8.3 % by weight) metallic element on the earth and its soluble form (Al^{3+}) is highly toxic to plant growth [10]. The toxicity of Al^{3+} induces damage of the central nervous system and is suspected in neurodegenerative diseases such as Alzheimer's and Parkinson's [11–13]. Thus, detection of Al^{3+} is crucial in monitoring and controlling the concentration levels in the biosphere and in reducing its harmful effects on human health.

To date, a number of analytical methods including ion selective electrodes [14, 15], voltammetric [16], atomic absorption spectrometry [17] and inductively coupled plasma mass spectrometry [18] play a role in the detection of metal ions. However, these methods are time-consuming and expensive, as they require tedious sample pretreatment and sophisticated experimental instrumentation and performance. Recently, great attention has been paid to the development of fluorescent and colorimetric chemosensors for the detection of Zn^{2+} and Al^{3+} ions [19–22]. Compared to other methods, fluorescence detection offers several advantages, such as high sensitivity, simple instrumentation, facile analysis, intrinsic selectivity, the capacity for rapid and real-time monitoring.

Fluoride plays an important role in biological, medical and chemical processes as the most electronegative atom, and the

smallest anion with high charge density [23–26]. Fluoride is a useful additive in toothpaste and in drinking water for the prevention of dental caries. However, excess of fluoride can result in fluorosis, urolithiasis, and cancer [27–32]. Therefore, precise determination of fluoride in samples is necessary.

Herein, we reports the synthesis of a new “turn on” fluorescent sensor based on bisphenol A-quinoline (BFQ) and its cation and anion binding properties by means of UV–vis, fluorescence and ^1H NMR spectroscopy. BFQ shows excellent selectivity for recognizing Zn^{2+} and Al^{3+} cations in EtOH– H_2O ($v/v=9/1$) and F^- anion in MeCN.

Experimental

General

Melting points were determined on an Electrothermal 9100 apparatus in a sealed capillary and were uncorrected. ^1H , ^{13}C , APT, COSY NMR spectra were recorded at room temperature on a Varian 400 MHz spectrometer in d_6 -DMSO and CDCl_3 . FT-IR spectra was obtained on a Perkin Elmer Spectrum 100 FTIR spectrometer. UV–vis spectra were measured with a Perkin Elmer Lambda 25 spectrometer. Elemental analyses were performed using a Leco CHNS-932 analyzer. Analytical TLC was performed using Merck prepared plates (silica gel 60 F254 on aluminum). All reactions, unless otherwise noted, were conducted under nitrogen atmosphere. All starting materials and reagents were of standard analytical grade from Fluka, Merck, and Aldrich and used without further purification.

Synthesis of Compound 1

A solution of bisphenol A (0.5 g, 2.19 mmol) and hexamethylenetetramine (HMTA, 3.67 g, 26.28 mmol) in trifluoroacetic acid (50 mL) was refluxed for 24 h. Upon completion of the reaction, the mixture was cooled to room temperature and adding 1.0 M HCl (100 mL). Then, the resulting mixture was extracted with dichloromethane (100 mL). The organic layer was washed with water three times and saturated brine once, and dried over MgSO_4 . Removing the solvent after filtration afforded to give **1** as yellow oil. Yield: 75 %; ^1H NMR (400 MHz CDCl_3) 10.93 (s, 2H), 9.85 (s, 2H), 7.43 (s, 2H), 7.34 (d, 2H, $J=8.4$ Hz), 6.91 (d, 2H, $J=8.6$ Hz), 1.70 (s, 6H). ^{13}C NMR (100 MHz CDCl_3) 196.59, 159.91, 141.50, 136.04, 130.77, 119.98, 117.62, 41.70, 30.67; Anal. calcd for $\text{C}_{17}\text{H}_{16}\text{O}_4$: C, 71.82; H, 5.67. Found: C, 71.98; H, 5.75.

Synthesis of BFQ

A solution of compound **1** (0.50 g, 1.76 mmol) and 8-aminoquinoline (0.52 g, 3.61 mmol) in absolute ethanol (40 mL) was refluxed for 3 h. The mixture was cooled to room temperature. The orange precipitate was filtered-off, washed with ethanol and dried in vacuum to give BFQ as an orange solid. Yield: 82 %; Mp=178 °C; ^1H NMR (400 MHz $\text{DMSO-}d_6$) 13.84 (s, 2H), 9.09 (s, 2H), 8.95 (d, 2H, $J=2.32$ Hz), 8.41 (d, 2H, $J=7.21$ Hz), 7.89 (d, 2H, $J=7.21$ Hz), 7.73 (d, 2H, $J=6.70$ Hz), 7.58–7.67 (m, 6H), 7.29 (d, 2H, $J=6.70$ Hz), 6.92 (d, 2H, $J=8.76$ Hz), 1.69 (s, 6H). ^{13}C NMR (100 MHz $\text{DMSO-}d_6$) 164.91, 159.88, 151.01, 145.19, 142.21, 140.98, 136.66, 132.73, 130.29, 129.15, 127.26, 126.91, 122.55, 119.13, 118.60, 117.24, 41.70; Anal. calcd for $\text{C}_{35}\text{H}_{28}\text{N}_4\text{O}_2$: C, 78.34; H, 5.26; N, 10.44. Found: C, 78.48; H, 5.35; N, 10.87.

UV–vis and Fluorescence Experiments

The stock solutions of BFQ (1.0 mM) in EtOH– H_2O ($v/v=9/1$) and metal ions (10.0 mM) as perchlorate salts in H_2O and anions (10.0 mM) as tetrabutylammonium salts in MeCN were prepared. The volume of a solution of BFQ used in the experiments was 3.0 mL. Titration spectra were recorded by adding corresponding volume of cation or anion solutions to a solution of BFQ. Every titration was repeated at least twice until consistent values were obtained.

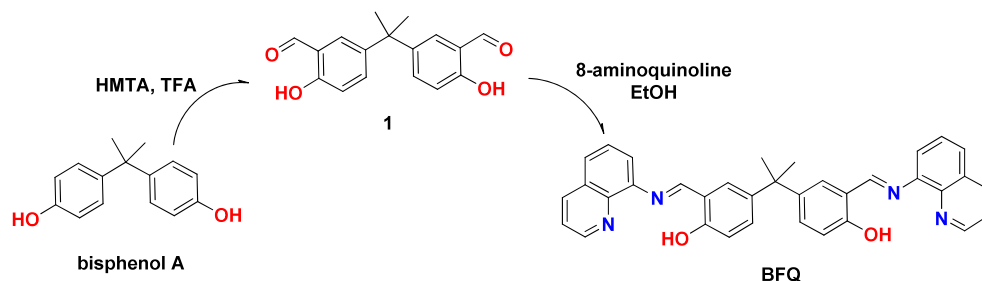
^1H NMR Titration Studies

^1H NMR titrations were performed on a Varian 400 MHz spectrometer at 298 K. A solution of BFQ (0.0663 M for $\text{Zn}^{2+}/\text{Al}^{3+}$ and 0.0540 M for F^- in $\text{DMSO-}d_6$) was titrated by adding known quantities of the concentrated solution of zinc/aluminum perchlorate and tetrabutylammonium fluoride (TBAF). The chemical shift changes of BFQ were monitored. All titrations were repeated at least twice to get the consistent values.

Results and Discussion

Synthesis of Chemosensor BFQ

A novel Schiff base derivative BFQ was easily synthesized via aldehyde–amine condensation reaction as depicted in Scheme 1. Firstly, the dialdehyde derivative of bisphenol A (**1**) was synthesized by Duff reaction in the presence of bisphenol A and hexamethylenetetramine (HMTA) in trifluoroacetic acid (TFA). Then, compound **1** was reacted with 8-aminoquinoline ethanol under reflux for 24 h to give BFQ in 82 % yield. The formation of BFQ was confirmed by

Scheme 1 Synthesis of chemosensor **BFQ**

the disappearance of aldehyde signal (CHO) at δ 9.85 ppm in compound **1** and by the appearance of imine signal (CHN) at δ 9.09 ppm in ^1H NMR spectra. The formation of imine bond was supported by the appearance of imine band (CH=N) at 1616 cm^{-1} in FTIR spectra. Also, the molecular structure of **BFQ** was confirmed by ^{13}C NMR, COSY, APT and elemental analysis (Supplementary data, Fig. S1–S7).

Cation-Sensing Properties of **BFQ**

To evaluate the selectivity and sensitivity of **BFQ** toward various cations, fluorescence spectra of **BFQ** were measured in the presence of nineteen cations: Li^+ , Na^+ , Cs^+ , Ag^+ , Ca^{2+} , Mg^{2+} , Sr^{2+} , Ba^{2+} , Hg^{2+} , Zn^{2+} , Ni^{2+} , Cu^{2+} , Cd^{2+} , Co^{2+} , Mn^{2+} , Pb^{2+} , Fe^{2+} , Fe^{3+} and Al^{3+} . Only Zn^{2+} and Al^{3+} caused the enhanced yellow and green emission, respectively. Because **BFQ** exhibited good solubility in various organic and polar solvents, we tested various solvents to select a proper detection media for the interaction of Zn^{2+} or Al^{3+} with **BFQ**. In the fluorescence spectra of the Zn^{2+} and Al^{3+} ions, **BFQ** exhibited good sensitivity in EtOH (Fig. S8). Aqueous media are essential for monitoring environmental, biological, and industrial samples. Thus we added in varying quantities of H_2O to

EtOH solution achieving ratios of 9:1–1:9 as indicated in Fig. S9. The optimum emission spectra were observed at an EtOH: H_2O ratio of 9:1 (v/v). Further studies were realized in EtOH- H_2O medium ($v/v=9/1$). The fluorescence behavior of **BFQ** was investigated in the presence of 10-fold excess of various metal ions in EtOH- H_2O ($v/v=9/1$) at room temperature. As shown in Fig. 1a, **BFQ** has a very weak fluorescence emission at 550 nm due to isomerization of the C=N double bond and effect of intramolecular charge transfer (ICT) in **BFQ**. The C=N isomerization and ICT effect in **BFQ** may be inhibited upon the coordination of **BFQ** to Zn^{2+} and Al^{3+} . Also it forms a rigid conjugation system, causing the CHEF (chelation enhanced fluorescence) effect [20, 21]. Thus, Zn^{2+} and Al^{3+} treatment resulted in a remarkably intensity increase at 560 and 530 nm, respectively. In contrast no fluorescence enhancement was detected after adding other metal ions including Li^+ , Na^+ , Cs^+ , Ag^+ , Ca^{2+} , Mg^{2+} , Sr^{2+} , Ba^{2+} , Hg^{2+} , Ni^{2+} , Cu^{2+} , Cd^{2+} , Co^{2+} , Mn^{2+} , Pb^{2+} , Fe^{2+} , and Fe^{3+} . The addition of Zn^{2+} and Al^{3+} to **BFQ** resulted in 13- and 17-fold increase in fluorescence intensities at 560 and 530 nm, respectively (Fig. 1b).

The fluorescence titrations were carried out by adding the increasing amounts of Zn^{2+} and Al^{3+} to a solution of **BFQ**,

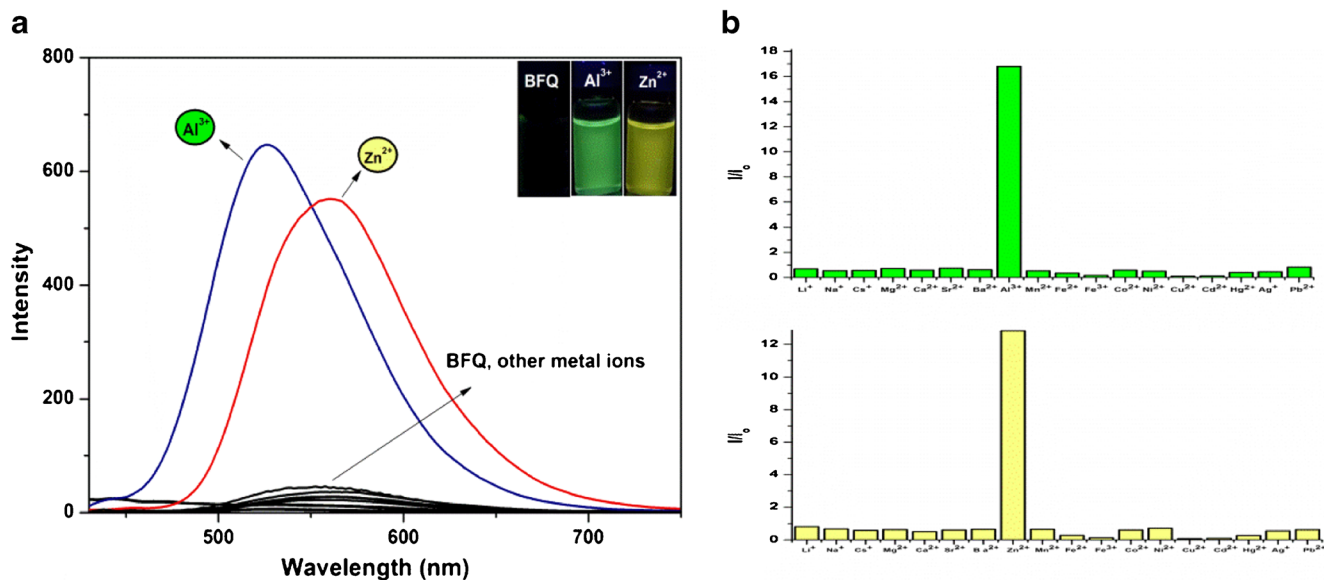


Fig. 1 Fluorescence spectra (a) and fluorescence intensities (b) at 530 and 560 nm of **BFQ** (10 μM) in EtOH- H_2O ($v/v=9/1$) in the presence of various cations (10.0 equiv.) ($\lambda_{\text{ex}}=395\text{ nm}$)

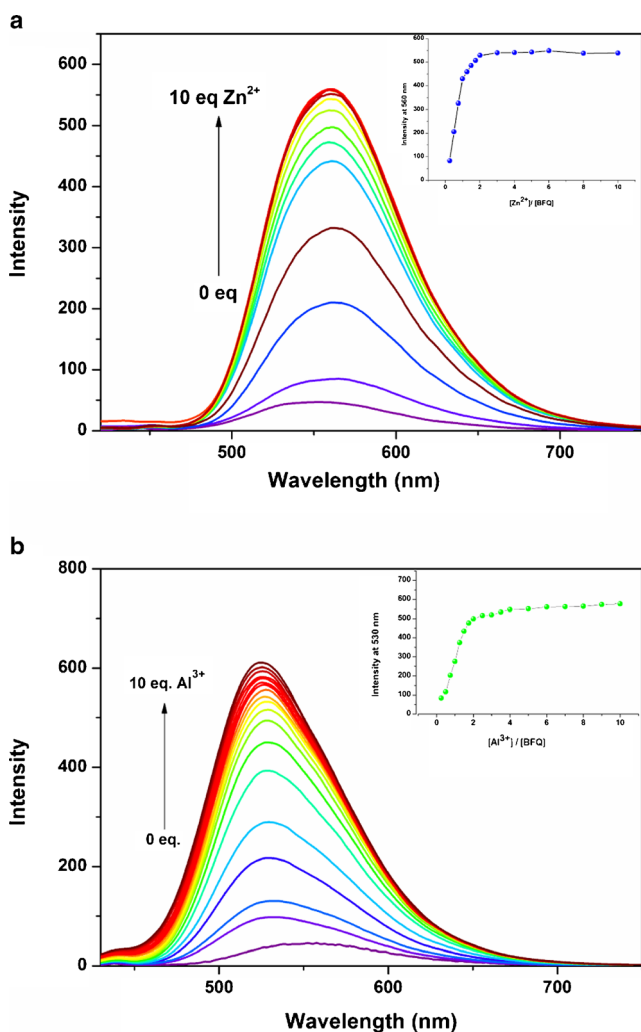


Fig. 2 Fluorescence response of **BFQ** (10 μM) with the addition of various amounts of Zn^{2+} (a) and Al^{3+} (b) in EtOH-H₂O ($v/v=9/1$)

and remarkable fluorescence enhancement was observed (Fig. 2a, b). When **BFQ** was titrated with Zn^{2+} ions, the emission band was shifted to ~560 nm with emission intensity enhancement. While in case of Al^{3+} ion, blue shift of the emission maxima (~550 to ~530 nm) was observed with increase in emission intensity with respect to the free **BFQ**. The emission intensities were stabilized after the amount of Zn^{2+} and Al^{3+} ions reached 10 equiv. with a defined emission point. To understand the binding stoichiometries of **BFQ**- Zn^{2+} and **BFQ**- Al^{3+} complexes, we realized Job plot experiments. In Fig. 3a, b, the emission intensities at 530 and 560 nm are plotted against the molar fractions of **BFQ**. Maximum emission intensities were measured for molar fractions of 0.33 and 0.36 showing complex formation between **BFQ**- Zn^{2+} and **BFQ**- Al^{3+} in 1:2 ratios. The association constants (K_a) by using fluorescence titration data are calculated to be $(8.51 \pm 0.25) \times 10^{10} M^{-2}$ for Zn^{2+} and $(1.53 \pm 0.18) \times 10^{10} M^{-2}$ for Al^{3+} according to Benesi-Hildebrand plot [33] (Fig. S10). Fluorimetric titration data were also used to obtain the detection limit of **BFQ** as a fluorescent sensor for the analysis of Zn^{2+} and Al^{3+} in a micromolar level and found to be $(3.56 \pm 0.14) \times 10^{-6} M$ and $(1.14 \pm 0.11) \times 10^{-6} M$, respectively (based on $S/N=3$) (Fig. S11). Moreover, the quantum yield (Φ) measurements for **BFQ**- Zn^{2+} and **BFQ**- Al^{3+} complexes were carried out at different concentrations in EtOH-H₂O ($v/v=9/1$) (Fig. S12). **BFQ** exhibited a weak and broad emission band with the quantum yield of $\Phi_{BFQ}=0.0107$. As the concentration of Zn^{2+} and Al^{3+} ion was increased, a remarkable emission enhancement at 560 and 530 nm was observed, respectively. The binding of Zn^{2+} and Al^{3+} to **BFQ** results in a chelation enhancement of fluorescence effect (CHEF), thus causing a remarkable enhancement in the emission intensity. Upon complexation, the quantum yields of **BFQ**- Zn^{2+} and **BFQ**- Al^{3+} reach $\Phi_{BFQ-Zn^{2+}}=0.172$ (about 16 fold) and $\Phi_{BFQ-Al^{3+}}=0.239$ (about 22 fold). Hence, the apparent color

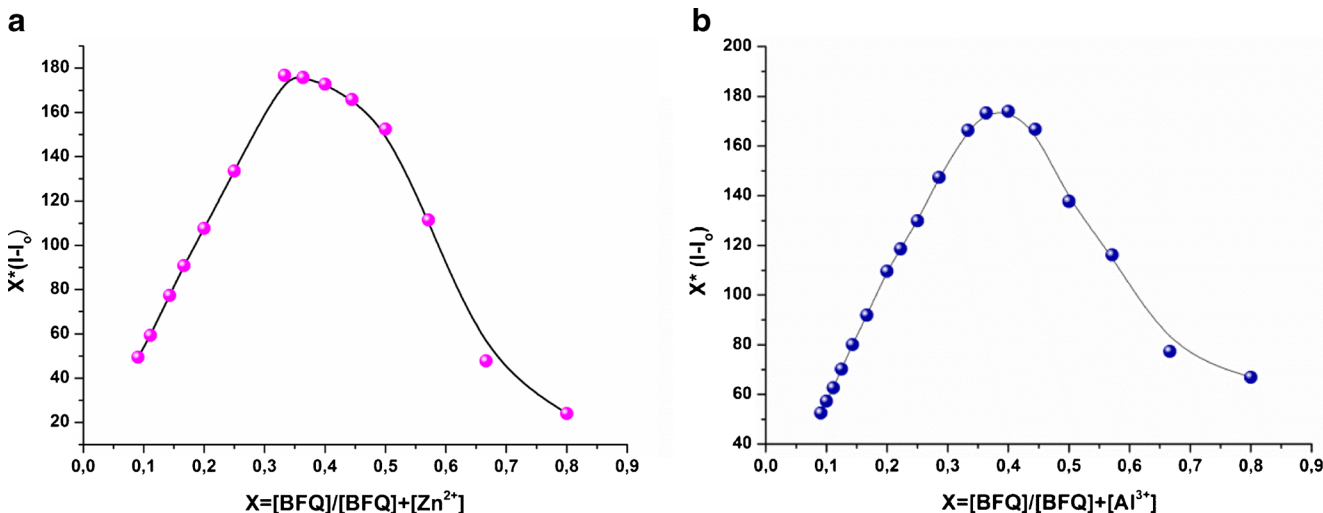


Fig. 3 Job's plots for determining the stoichiometric complexation of **BFQ** with Zn^{2+} (a) and Al^{3+} (b) in EtOH-H₂O ($v/v=9/1$)

Table 1 Photophysical properties of sensor complexes

Sensor complexes	Excitation wavelength (nm, λ_{ex})	Emission wavelength (nm, λ_{em})	Association constants (K_a , M^{-2})	Detection limits (M)	Quantum Yield (Φ)
BFQ-Zn²⁺	395	560	^a $(8.51 \pm 0.25) \times 10^{10}$ ^b $(2.32 \pm 0.21) \times 10^{10}$	$(3.56 \pm 0.14) \times 10^{-6}$	0.172
BFQ-Al³⁺	395	530	^a $(1.53 \pm 0.18) \times 10^{10}$ ^b $(0.73 \pm 0.17) \times 10^{10}$	$(1.14 \pm 0.11) \times 10^{-6}$	0.239
BFQ-F⁻	420	610	^b $(8.37 \pm 0.17) \times 10^8$	$(3.68 \pm 0.21) \times 10^{-6}$	0.118

^a Fluorescence method, ^b UV–vis method, Conditions; T=298 K; EtOH-H₂O ($v/v=9/1$) for Zn²⁺/Al³⁺ and MeCN for F⁻

changes from colorless to yellow for Zn²⁺ and green for Al³⁺ are observed during the detection process. Photophysical properties of sensor complexes were also summarized in Table 1.

The interaction of **BFQ** with Zn²⁺ and Al³⁺ ions was further investigated through UV–vis titration in EtOH–H₂O ($v/v=9/1$) (Fig. 4a, b). Upon the addition of Zn²⁺ ions (0–5 equiv.) to a solution of **BFQ** (10 μ M), the absorption peak at 341 nm decreased while the absorption peak at 452 nm rapidly increased and shifted to 445 nm (Fig. 4a). By addition of Al³⁺ (0–5 equiv.) to a solution of **BFQ** (10 μ M), the absorption peaks at 341 and 452 nm belong to **BFQ** gradually decreased (Fig. 4b). The association constants of Zn²⁺ and Al³⁺ ions were calculated from UV–vis titration experiments by Benesi–Hildebrand plot [33] and found as $(2.32 \pm 0.21) \times 10^{10}$ and $(0.73 \pm 0.17) \times 10^{10} M^{-2}$, respectively (Fig. S13).

To utilize **BFQ** as a selective sensor for Zn²⁺ and Al³⁺, the effect of competing metal ions has been examined by recording the fluorescence spectra of **BFQ** (10 μ M) with Zn²⁺/Al³⁺ (10 equiv.) in the presence of a competing metal ion (20 equiv.). As seen in Fig. 5a, b, Zn²⁺ and Al³⁺ ions detection by **BFQ** is not influenced by the presence of other competing

metal ion. Thus, Zn²⁺ and Al³⁺ can be easily detected in the presence of most competing metal ions through fluorescence ‘turn on’ behavior.

The response time for many fluorescent sensors is an important factor. Thus, the effect of the reaction time on the binding process of Zn²⁺ and Al³⁺ ions to **BFQ** was investigated as shown in Fig. S14 (Supplementary data). Following the addition of 10 equiv. Zn²⁺ and 10 equiv. Al³⁺ ions to 10 μ M **BFQ**, the fluorescence intensity of **BFQ** was reached a stable value within 1 min and remaining constant from 1 to 10 min. The rapid, stable complexation of Zn²⁺ and Al³⁺ ions by **BFQ** and the resulting quick response profile are important features for robust, real time detection of Zn²⁺ and Al³⁺ ions by portable device in field.

To understand the nature of interaction between **BFQ** and Zn²⁺/Al³⁺, ¹H NMR titration experiments were carried out in *d*₆-DMSO. The addition of 2.0 equiv. of Zn²⁺ and Al³⁺ to a solution of **BFQ** in *d*₆-DMSO resulted in different peak profiles (Fig. 6). The phenolic-OH signal (H_a) at 13.84 ppm disappeared upon the addition of Zn²⁺ and Al³⁺ ions to a **BFQ** solution. The ortho-proton signal (H_c) at 8.95 ppm belongs to quinolone moiety of **BFQ** was downfield shifted to

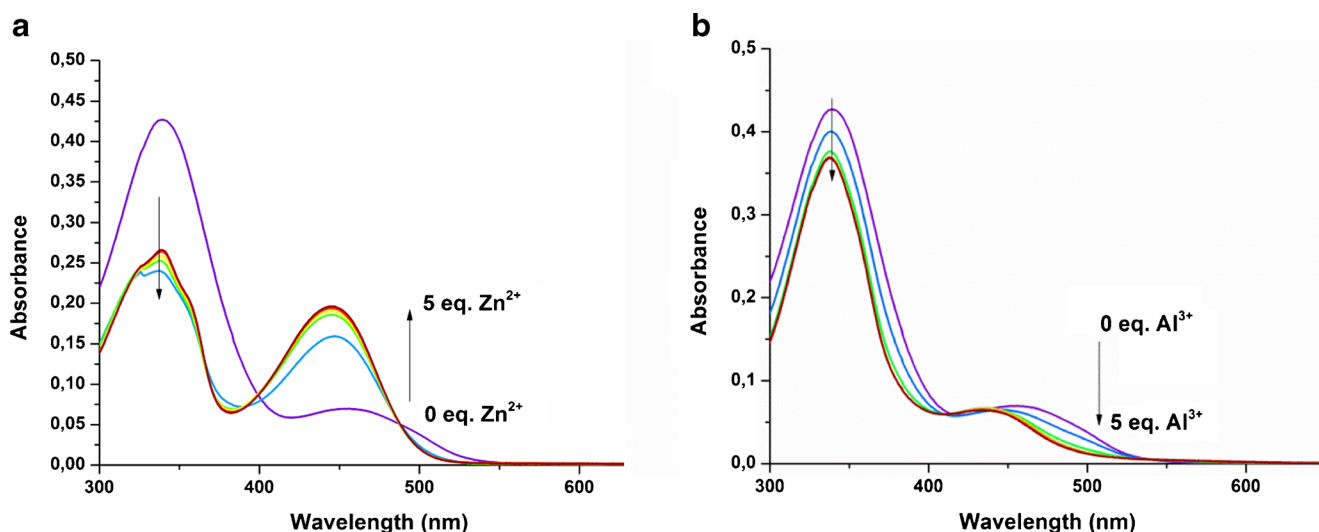


Fig. 4 Absorption spectra of **BFQ** (10 μ M) upon addition of different concentrations of Zn²⁺ (a) and Al³⁺ (b) in EtOH–H₂O ($v/v=9/1$)

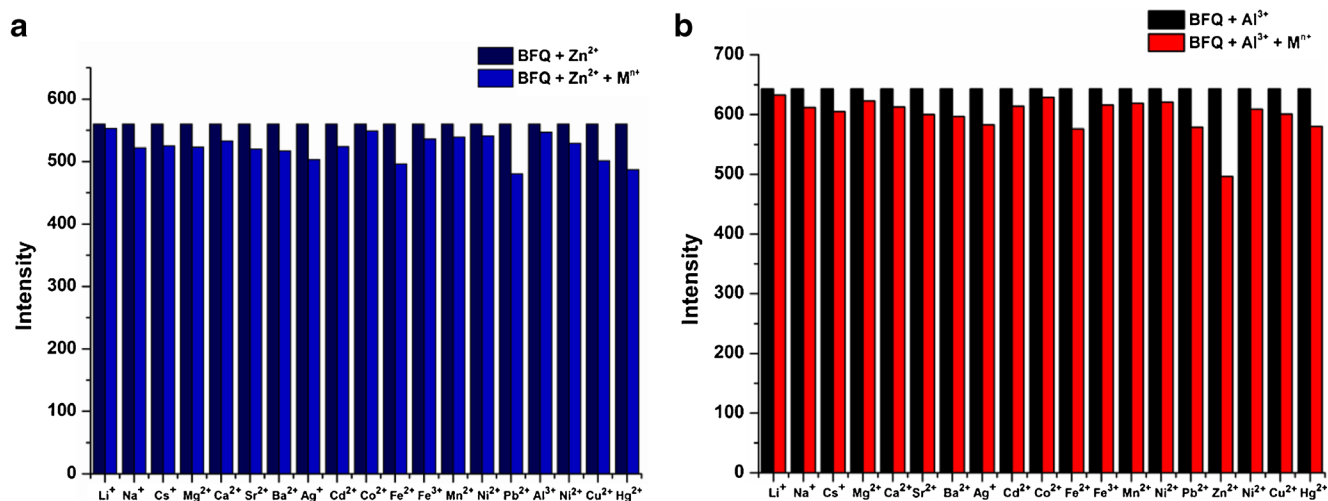


Fig. 5 Relative fluorescence intensities of **BFQ** (10 μM) in EtOH-H₂O (v/v=9/1) with 10 equiv. Zn²⁺ (a) and 10 equiv. Al³⁺ (b) in the presence or absence of other competition metal ions (20 equiv.)

10.21 ppm for Al³⁺ and to 10.22 ppm for Zn²⁺. Similarly, Schiff base proton signal (H_b) at 9.08 ppm was downfield shifted to 10.64 ppm for Al³⁺ and 10.63 ppm for Zn²⁺, respectively, suggesting N-metal coordination. In addition, other aromatic proton signals became more complicated. These results imply that the phenolic-OH, Schiff base and quinoline-N groups are efficient on formation of complex between the **BFQ** and Zn²⁺/Al³⁺.

Anion-Sensing Properties of **BFQ**

The receptors with the imine and phenol groups show the sensing properties of anions sometimes [34–36]. Therefore, the anion-sensing properties of **BFQ** were examined in the presence of 40-fold excess of various anions in MeCN at room temperature. The results indicated that fluoride ion has preferential interaction with **BFQ** in MeCN. As shown in Fig. 7,

BFQ exhibited a very weak fluorescence emission with an excitation of 420 nm in MeCN. The addition of various anions such as NO₃⁻, ClO₄⁻, HSO₄⁻, H₂PO₄⁻, AcO⁻, Cl⁻, Br⁻, and I⁻ to the **BFQ** solution showed no enhancement in the emission intensity. In contrast, there was a selective fluorescent enhancing effect (35-fold) in its emission spectrum with only F⁻ ion at 610 nm. In order to study the binding interaction of **BFQ** and F⁻, the fluorescence titration experiments were realized (Fig. 8). As the F⁻ concentration increased, the emission intensity increased drastically and reached saturation when 40 equiv. of F⁻ was added. In order to determine the stoichiometric ratio between **BFQ** and F⁻, the method of continuous variation (Job's plot) was used. Fig. S15 shows the Job's plot of **BFQ** with F⁻. **BFQ**-F⁻ complex concentration approaches a maximum when the mole fraction of **BFQ** is 0.33, which means **BFQ** and F⁻ form 1:2 complexes. On the basis of 1:2 stoichiometry, the association constant was calculated to be

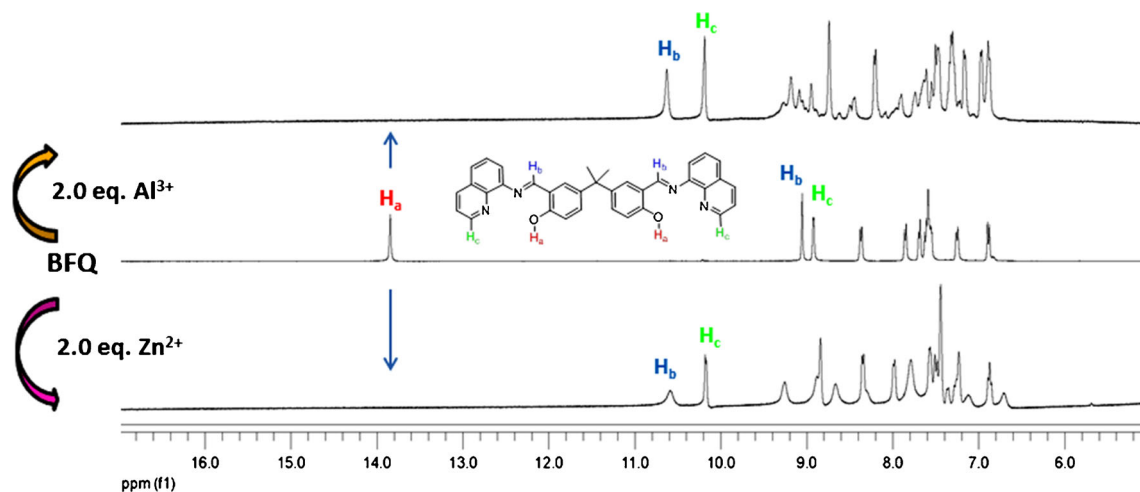


Fig. 6 ¹H NMR spectra of **BFQ** in the presence of 2.0 equiv. of Zn²⁺ and Al³⁺ in DMSO-*d*₆

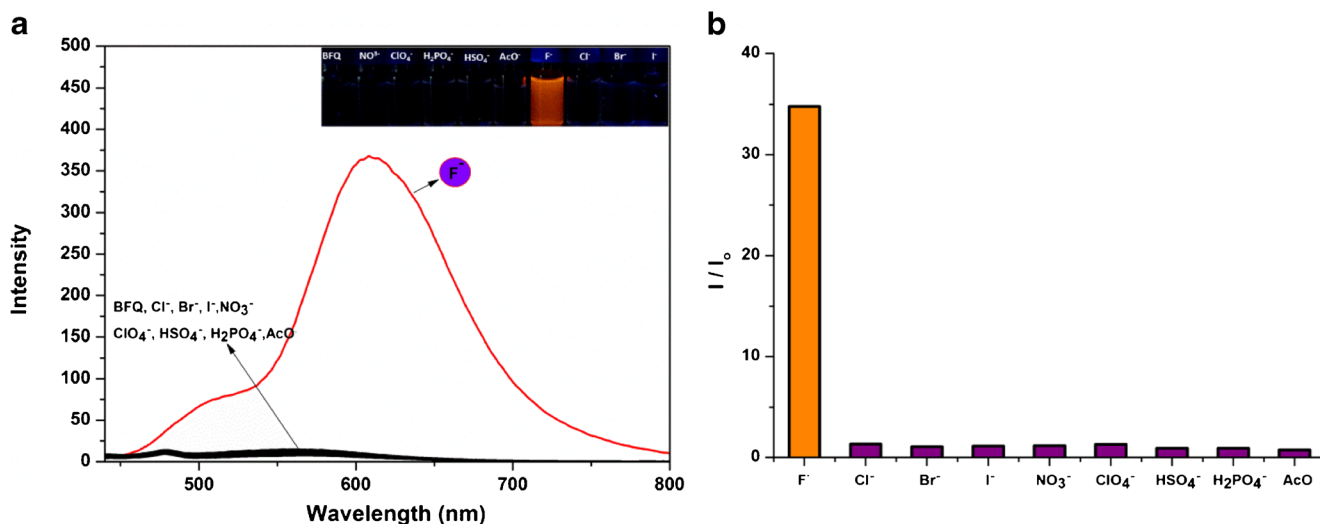


Fig. 7 (a) Fluorescence spectra of **BFQ** (10 μM) recorded in MeCN in the presence of various anions (40 equiv.). (b) Selective fluorescence enhancement of **BFQ** to F^- over other anions

$(8.37 \pm 0.17) \times 10^8 \text{ M}^{-2}$ for **BFQ**– F^- complex from the Benesi–Hildebrand equation (Fig. S16). The detection limit was also determined to be $(3.68 \pm 0.21) \times 10^{-6} \text{ M}$, based on the fluorescence titration measurement (Fig. S17). Furthermore, the quantum yield (Φ) for **BFQ**– F^- complex was measured in MeCN. **BFQ**– F^- ($\Phi=0.118$) complex demonstrated 30 times higher Φ value than that of **BFQ** ($\Phi=0.0061$) (Table 1, Fig. S18).

To understand the interaction between **BFQ** and F^- , UV–vis titration experiments were carried out in MeCN. Figure 9 shows the UV–vis absorption spectra of **BFQ** (10 μM) upon addition of different equiv. of F^- in MeCN. The absorption at 348 nm decreased and a new peak appeared at 445 nm upon increasing the concentration of F^- . An isosbestic point was

observed at 387 nm. Considering the large contribution of the electron density change for the conjugated system in the deprotonated **BFQ**, it could be concluded that the interaction was deprotonation rather than hydrogen bonding because of the significant absorption shift.

The ^1H NMR titration of **BFQ** was examined in the absence and the presence of F^- in $\text{DMSO}-d_6$ (Fig. 10). The phenolic-OH proton signal (H_a) at 13.84 ppm was disappeared upon the addition of 1.0 equivalent of F^- ion to a **BFQ** solution. The ortho-proton signal (H_c) at 8.95 ppm belongs to quinolone moiety and Schiff base proton signal (H_b) at 9.08 ppm were upfield shifted to 8.49 and 8.52 ppm, respectively, upon addition of 0–4.0 equiv. of F^- . The deprotonation of the phenolic-OH in **BFQ** also caused significant upfield

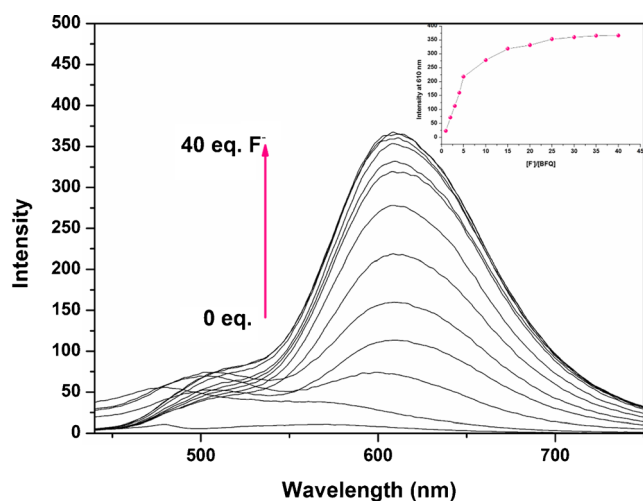


Fig. 8 Fluorescence spectra ($\lambda_{\text{ex}}=420 \text{ nm}$) of **BFQ** (10 μM) upon the addition of F^- in MeCN. (inset) Graph of the fluorescence intensity at 610 nm as a function of F^- concentration

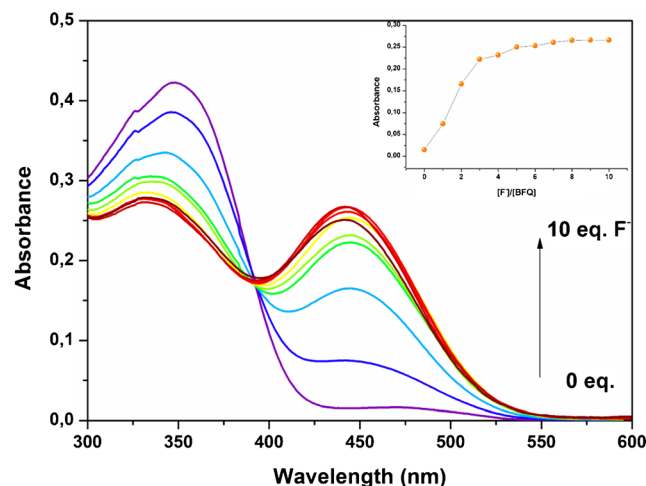


Fig. 9 UV–vis spectral changes of **BFQ** (10 μM) with the addition of 0.0–10.0 equiv. of F^- in MeCN

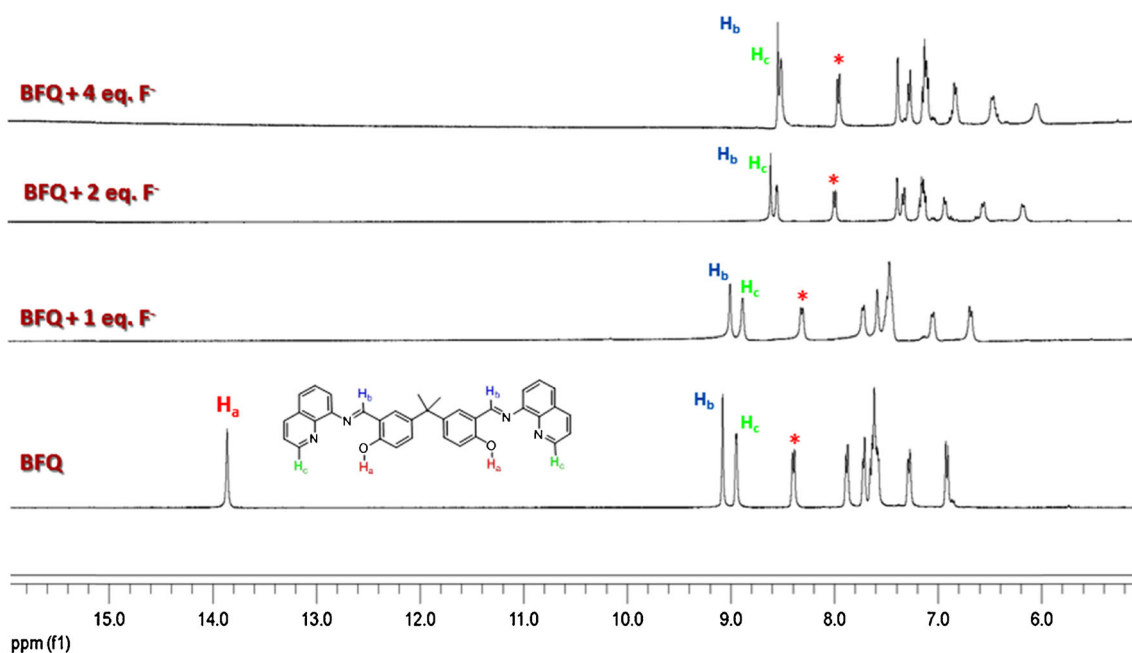


Fig. 10 ^1H NMR spectra of **BFQ** in the presence of 0–4.0 equiv. of TBAF in $\text{DMSO-}d_6$

shifts of the protons of benzene moiety due to the electron density on the phenyl rings with through bond propagation which generates a shielding effect [37, 38]. These results demonstrated the formation of a new complex between the phenolic-OH and fluoride.

Conclusion

In conclusion, a novel Schiff base derivative based bisphenol A-quinoline (**BFQ**) was easily synthesized in two-step, and was used as fluorescence “turn-on” sensors for distinct detections of Zn^{2+} , Al^{3+} and F^- ions. **BFQ** indicated fluorescence turn-on sensor responses to Zn^{2+} and Al^{3+} in $\text{EtOH-H}_2\text{O}$ ($v/v=9/1$) and F^- in MeCN. The stoichiometries of complexes (**BFQ-Zn** $^{2+}$, **BFQ-Al** $^{3+}$ and **BFQ-F** $^-$) were determined to be 1:2 from job’s plots based on UV–vis and fluorescence spectral changes. The detection limits (LODs) of **BFQ-Zn** $^{2+}$, **BFQ-Al** $^{3+}$ and **BFQ-F** $^-$ sensor complexes were calculated as 3.56, 1.14, and 3.68 μM , respectively, by standard deviations and linear fittings. This type of a highly sensitive and selective fluorescent sensor will be useful for development of new chemosensors for multiple targets such as cations and anions.

Acknowledgement We thank the Research Foundation of Selcuk University (SUBAP) for financial support of this work.

Compliance with Ethical Standards We state compliance with ethical standards of the present study, below.

Funding This study was funded by SUBAP.

Conflict of Interest We declare that they have no conflict of interest.

Research involving Human Participants and/or Animals This study does not contain any studies with human participants performed by any of the authors.

Informed consent For this study, any informed consent form was not obtained.

References

- Dong Z, Le X, Zhou P, Dong C, Ma J (2014) Sequential recognition of zinc ion and hydrogen sulfide by a new quinoline derivative with logic gate behavior. *R Soc Chem Adv* 4:18270–18277
- Dong Z, Le X, Zhou P, Dong C, Ma J (2014) An “off–on–off” fluorescent probe for the sequential detection of Zn^{2+} and hydrogen sulfide in aqueous solution. *New J Chem* 38:1802–1808
- Hatai J, Pal S, Jose GP, Sengupta T, Bandyopadhyay S (2012) A single molecule multi chemosensor differentiates among Zn^{2+} , Pb^{2+} and Hg^{2+} : modulation of selectivity by tuning of solvents. *R Soc Chem Adv* 2:7033–7036
- Malkondu S, Erdemir S (2014) A triphenylamine based multi-analyte chemosensor for Hg^{2+} and Cu^{2+} ions in MeCN/ H_2O . *Tetrahedron* 70:5494–5498
- Bergand JM, Shi Y (1996) The galvanization of biology: a growing appreciation for the roles of zinc. *Science* 271:1081–1085
- Xieand XM, Smart TG (1991) A physiological role for endogenous zinc in rat hippocampal synaptic neurotransmission. *Nature* 349:521–524

7. Torrado A, Walkupand GK, Imperiali B (1998) Exploiting polypeptide motifs for the design of selective Cu (II) Ion chemosensors. *J Am Chem Soc* 120:609–610
8. Jin T, Lu J, Nordberg M (1998) *Neuro Toxicol* 19:529–536
9. Bhalla V, Kumar R, Kumar M (2013) Pentaquinone based probe for nanomolar detection of zinc ions: Chemosensing ensemble as an antioxidant. *Dalton Trans* 42:975–980
10. Delhaizeand E, Ryan PR (1995) Aluminum toxicity and tolerance in plants. *Plant Physiol* 107:315–321
11. Andrasi E, Pali N, Molnar Z, Kosel S (2005) Brain aluminum, magnesium and phosphorus contents of control and Alzheimer-diseased patients. *J Alzheimers Dis* 7(273):284
12. Nayak P (2002) Aluminum: impacts and disease. *Environ Res* 89: 101–115
13. Berthon G (2002) Aluminum speciation in relation to aluminum bioavailability, metabolism and toxicity. *Coord Chem Rev* 228: 319–341
14. Gupta VK, Yola ML, Atar N, Solak AO, Uzun L, Ustundag Z (2013) Electrochemically modified sulfisoxazolenano film on glassy carbon for determination of cadmium (II) in water samples. *Electrochim Acta* 105:149–156
15. Gupta VK, Singh AK, Singh P, Upadhyay A (2014) Electrochemical determination of perchlorate ion by polymeric membrane and coated graphite electrodes based on zinc complexes of macrocyclic ligands. *Sensors Actuators B* 199:201–209
16. Norouzi P, Gupta VK, Larijani B, Rasoolipour S, Faridbod F, Ganjali MR (2015) Coulometric differential FFT admittance voltammetry determination of amlodipine in pharmaceutical formulation by nano-composite electrode. *Talanta* 131:577–584
17. Iyengar V, Wolttlez J (1988) Trace elements in human clinical specimens: evaluation of literature data to identify reference values, trace elements in human clinical specimens: evaluation of literature data to identify reference values. *Clin Chem Wash DC* 34:474–481
18. Townsend AT, Miller KA, McLean S, Aldous S (1998) The determination of copper, zinc, cadmium and lead in urine by high resolution ICP-MS. *J Anal At Spectrom* 13:1213–1219
19. Alici O, Erdemir S (2015) A cyanobiphenyl containing fluorescence “turn on” sensor for Al^{3+} ion in CH_3CN -water. *Sensors Actuators B Chem* 208:159–163
20. Erdemir S, Malkondu S (2015) A simple triazole-based “turn on” fluorescent sensor for Al^{3+} ion in $MeCN-H_2O$ and F^- ion in $MeCN$. *J Luminescence* 158:401–406
21. Erdemir S, Malkondu S (2013) A novel “turn on” fluorescent sensor based on hydroxy-triphenylamine for Zn^{2+} and Cd^{2+} ions in $MeCN$. *Sens. Actuators B Chem* 188:1225–1229
22. Tayadea K, Sahoo SK, Bondhopadhyayd B, Bhardwajc VK, Singhc N, Basud A, Bendrea R, Kuwara A (2014) Highly selective turn-on fluorescent sensor for nanomolar detection of biologically important Zn^{2+} based on isonicotinohydrazide derivative: application in cellular imaging. *Biosens Bioelectron* 61:429–433
23. Zhang G, Wang L, Cai X, Zhang L, Yu J, Wang A (2013) A new diketopyrrolopyrrole (DPP) derivative bearing boronate group as fluorescent probe for fluoride ion. *Dyes Pigm* 98:232–237
24. Ghosh K, Kar D, Fröhlich R, Chattopadhyay AP, Samaddera A, Khuda-Bukhsh AR (2013) O-tert-butylidiphenyl silyl coumarin and dicoumarol: a case toward selective sensing of F^- ions in organic and aqueous environments. *Analyst* 138:3038–304
25. Luxami V, Kumar S (2007) Colorimetric and ratiometric fluorescence sensing of fluoride ions based on competitive intra- and intermolecular proton transfer. *Tetrahedron Lett* 48:3083–3087
26. Im HG, Kim HY, Choia MG, Chang SK (2013) Reaction-based dual signaling of fluoride ions by sulfonates. *Org Biomol Chem* 11:2966–2971
27. Carton RJ (2006) Fluoride. Review of the 2006 United States National Research Council Report: Fluoride in Drinking. *Water* 39: 163–172
28. Arhima MH, Gulatiand OP, Sharma SC (2004) The effect of Pycnogenol on fluoride induced Rat kidney lysosomal damage in vitro. *Phytother Res* 18:244–246
29. Matsui H, Morimoto M, Horimotoand K, Nishimura Y (2007) Some characteristics of fluoride-induced cell death in rat thymocytes: cytotoxicity of sodium fluoride. *Toxicol In Vitro* 21:1113–1120
30. Horowitz HS (2003) The 2001 CDC recommendations for using fluoride to prevent and control dental caries in the United States. *J Public Health Dent* 63:3–8
31. Ayooband S, Gupta AK (2006) Fluoride in drinking water: a review on the status and stress effects. *Crit Rev Environ Sci Technol* 36: 433–487
32. Bassin E, Wypij D, Davisand R, Mittleman M (2006) Age-specific fluoride exposure in drinking water and osteosarcoma (United States). *Cancer Causes Control* 17:421–428
33. Benesi HA, Hildebrand JH (1949) A spectrophotometric investigation of the inter-action of iodine with aromatic hydrocarbons. *J Am Chem Soc* 71:2703–2707
34. Sharma D, Sahoo SK, Bera RK, Kamal R (2013) Spectroscopic and computational study of a naphthalene derivative as colorimetric and fluorescent sensor for bioactive anions. *J Fluoresc* 23:387–392
35. Sharma D, Moirangthem A, Sahoo SK, Basu A, Roy SM, Pati RK, Kumar SKA, Nandre JP, Patil UD (2014) Anion selective chromogenic and fluorogenic chemosensor and its application in breast cancer live cell imaging. *RSC Adv* 4:41446–41452
36. Sivakumar R, Reena V, Ananthi N, Babu M, Anandan S, Velmathi S (2010) Colorimetric and fluorescence sensing of fluoride anions with potential salicylaldehyde based schiff base receptors. *Spectrochim Acta A Mol Biomol Spectrosc* 75:1146–1151
37. Peng X, Wu Y, Fan J, Tian M, Han K (2005) Colorimetric and ratiometric fluorescence sensing of fluoride: tuning selectivity in proton transfer. *J Org Chem* 70:10524–10531
38. Erdemir S, Kocyigit O, Alici O, Malkondu S (2013) ‘Naked-eye’ detection of F^- ions by two novel colorimetric receptors. *Tetrahedron Lett* 54:613–617